

Communication

Performance of Orbital Angular Momentum Communication for a Non-Uniformly Correlated High-Order Bessel–Gaussian Beam in a Turbulent Atmosphere

Zihan Cong ^{1,2,3}, Hui Zhang ^{1,2,3}, Yaru Gao ^{1,2,3}, Yangjian Cai ^{1,2,3,*} and Yangsheng Yuan ^{1,2,3,*}

¹ Shandong Provincial Engineering and Technical Center of Light Manipulations & Shandong Provincial Key Laboratory of Optics and Photonic Device, School of Physics and Electronics, Shandong Normal University, Jinan 250014, China; 2021317050@stu.sdnu.edu.cn (Z.C.); 2020010068@stu.sdnu.edu.cn (H.Z.); gaoyaru@sdnu.edu.cn (Y.G.)

² Collaborative Innovation Center of Light Manipulation and Applications, Shandong Normal University, Jinan 250358, China

³ Joint Research Center of Light Manipulation Science and Photonic Integrated Chip of East China Normal University and Shandong Normal University, East China Normal University, Shanghai 200241, China

* Correspondence: yangjiancai@sdnu.edu.cn (Y.C.); yysheng@sdnu.edu.cn (Y.Y.)

Abstract: We derived the formula for the detection probability, signal-to-noise ratio (SNR), and average bit error rate (BER) for the signal orbital angular momentum (OAM) state carried via non-uniformly correlated high-order Bessel–Gaussian beam propagation in a turbulent atmosphere. The wavelength, receiver aperture, beam width, strength of the turbulent atmosphere, and topological charge effect on detection probability, SNR, and average BER of the signal OAM state were demonstrated numerically. The results show that the signal OAM state with low topological charge, a small receiver aperture, a narrow beam width, and a long wavelength can improve the performance of optical communications systems under conditions of weak atmospheric turbulence. Our results will be useful in long-distance free space optical (FSO) communications.

Citation: Cong, Z.; Zhang, H.; Gao, Y.; Cai, Y.; Yuan, Y. Performance of Orbital Angular Momentum Communication for a Non-Uniformly Correlated High-Order Bessel–Gaussian Beam in a Turbulent Atmosphere. *Photonics* **2024**, *11*, 131. <https://doi.org/10.3390/photonics11020131>

Received: 27 December 2023

Revised: 21 January 2024

Accepted: 29 January 2024

Published: 30 January 2024



Copyright: © 2024 by the authors. Licensee MDPI, Basel, Switzerland. This article is an open access article distributed under the terms and conditions of the Creative Commons Attribution (CC BY) license (<https://creativecommons.org/licenses/by/4.0/>).

Keywords: free space optical communications; turbulent atmosphere; detection probability; signal-to-noise ratio; bit error rate

1. Introduction

Orbital angular momentum (OAM) communication has broad application prospects in FSO communications [1–5]. The OAM modes carried by vortex beams have theoretically infinite eigenmodes and can form an infinite-dimensional Hilbert space, which can be used in FSO communications to increase capacity and spectral efficiency via the mode-division multiplexing technique. The vortex beam carrying the OAM mode inevitably encounters atmospheric turbulence when it propagates in free space. The initial OAM state will be degraded by atmospheric turbulence, followed by the OAM mode's crosstalk generation for the power of it spreading to the neighboring OAM states [6–11]. Therefore, the phase of the vortex beams is perturbed by atmospheric turbulence, the detection probability of the signal OAM state decreases [12], the signal-to-noise ratio (SNR) decreases, [13] and the bit error rate (BER) [14–18] increases. These are important parameters for evaluating the performance of FSO communication systems.

The performance of communication channels in a turbulent atmosphere can be improved by employing partially coherent beams [19–21]. In the past few decades, the propagation properties of the many types of partially coherent beams, for example, the Gaussian–Schell beam [22], partially coherent rectangular array beams [23], the Gaussian–Schell model vortex beam [24], partially coherent radially polarized beams [25], Airy–Schell

beams [26], partially coherent four-petal elliptic Gaussian vortex beams [27], partially coherent beams carrying a cross phase [28], and partially coherent twisted Gaussian beams [29] have been researched and used to mitigate the effects of a turbulent atmosphere on the signal quality of FSO communications.

Non-uniformly correlated beams with spatially varying coherence are different from the Schell-model beams with uniform coherence distributions [30–34]. The characteristics of non-uniformly correlated beams can be used to measure the refractive indices of a uniaxial crystal based on its independent self-focusing property along the propagation directions [35]. Two high-index particles were trapped simultaneously and manipulated in the longitudinal direction via focused structured optical fields with a spatially non-uniform correlation [36]. Non-uniformly correlated beams can also be used to resist the negative effects induced by atmospheric turbulence [37–42]. The research results show that the scintillation of Gaussian non-uniformly correlated beams and Hermite non-uniformly correlated beams was lower than that of the Gaussian–Schell model beams [37,38]. The power-in-the-bucket value can be enhanced under conditions of weakly anisotropic turbulence by controlling the coherence parameter for non-uniformly correlated beams [39]. In one study, convex partially coherent flat-topped beams were used to improve the mean SNR and reduce the mean BER [40]. Laguerre non-uniformly correlated beams with a suitable beam order and coherence length were applied to reduce the detrimental effect caused by atmospheric turbulence [41]. The fiber-coupling efficiency of the Laguerre non-uniformly correlated beam was better than that of the conventional Gaussian–Schell-model beam in FSO communications [42]. Therefore, non-uniformly correlated high-order Bessel–Gaussian beams carrying the OAM state can be applied to improve the performance of OAM communications in FSO communications.

In this study, we theoretically investigated the OAM state carried by non-uniformly correlated high-order Bessel–Gaussian beams disturbed by a turbulent atmosphere. The detection probability, SNR, and BER equation of the signal OAM states for non-uniformly correlated high-order Bessel–Gaussian beam propagation in a turbulent atmosphere were derived according to its intensity distribution at the receiver plane. The results show that the performance of OAM communications can be enhanced by non-uniformly correlated high-order Bessel–Gaussian beams. Our results will be useful in FSO communications.

2. Theory

Cross-spectral density (CSD) was used to characterize the partially coherent beams, which can be described at the source plane ($z = 0$) as follows:

$$W_0(r_1, r_2, \theta_1, \theta_2, 0) = \langle E^*(r_1, \theta_1) E(r_2, \theta_2) \rangle \quad (1)$$

Here, (r, θ) are the polar coordinates, $E(r, \theta)$ denotes the electric field of the beam, the angular brackets $\langle \cdot \rangle$ indicate the ensemble average, and the asterisk denotes the complex conjugate. In general, mode representation is applied to express the CSD of the beam as follows:

$$W_0(r_1, r_2, \theta_1, \theta_2, 0) = \int p(v) H(r_1, \theta_1, v) H^*(r_2, \theta_2, v) dv \quad (2)$$

Here, v is the corresponding vector in Fourier space of a position vector r in the polar coordinate system. The evolution properties of the OAM state for a non-uniformly correlated high-order Bessel–Gaussian beam can be derived from the functions of $p(v)$ and $H(r, \theta, v)$. Then, a non-negative function $p(v)$ is expressed as

$$p(v) = \frac{1}{\sqrt{\pi a}} \exp\left(-\frac{v^2}{a^2}\right) \quad (3)$$

and the kernel with an arbitrary function for the equation $H(r, \theta, v)$ is described as

$$H(r, \theta, v) = J_{l_0}(\alpha r) \exp\left(-\frac{r^2}{w_0^2}\right) \exp(-ikvr^2) \exp(il_0\theta) \quad (4)$$

where the parameter $a = 2 / kr_c^2$ is a positive real constant with a coherence length of r_c , $k = 2\pi / \lambda$ is a wavenumber with a wavelength of λ , l_0 is the topological charge of the OAM state, J_{l_0} is the l_0 -th order Bessel function of the first kind, α is a radial wave vector, and w_0 is the waist width of the Gaussian beam.

Substituting Equations (3) and (4) into Equation (2), the CSD of the non-uniformly correlated high-order Bessel–Gaussian beam at the source plane can be obtained as follows:

$$\begin{aligned} &W_0(r_1, r_2, \theta_1, \theta_2, 0) \\ &= J_{l_0}(\alpha r_1) J_{l_0}(\alpha r_2) \exp\left(-\frac{r_1^2 + r_2^2}{w_0^2}\right) \exp\left[-\frac{(r_2^2 - r_1^2)^2}{r_c^4}\right] \exp[-il_0(\theta_1 - \theta_2)] \end{aligned} \quad (5)$$

Here, $r_c = \sqrt{2 / ka}$ is the coherence length.

According to the Huygens–Fresnel principle and paraxial approximation, the field in the receiver plane of the CSD function of non-uniformly correlated high-order Bessel–Gaussian beams in free space without a turbulent atmosphere can be obtained as follows:

$$\begin{aligned} W(\rho_1, \rho_2, \varphi_1, \varphi_2, z) &= \frac{k^2}{4\pi^2 z^2} \iiint \iiint W_0(r_1, r_2, \theta_1, \theta_2, 0) \\ &\times \exp\left\{-\frac{ik}{2z} [r_1^2 - r_2^2 - 2r_1\rho_1 \cos(\theta_1 - \varphi_1) + 2r_2\rho_2 \cos(\theta_2 - \varphi_2)]\right\} r_1 r_2 dr_1 dr_2 d\theta_1 d\theta_2 \end{aligned} \quad (6)$$

Here, (ρ, φ) are the polar coordinates in the receiver plane. When a non-uniformly correlated high-order Bessel–Gaussian beam propagates through a turbulent atmosphere, the evolution properties of the OAM states of this beam are influenced by atmospheric turbulence, the purity of the OAM mode decreases, and the crosstalk increases. To conveniently analyze the purity and crosstalk of the OAM modes, the parameter $\rho_1 = \rho_2 = \rho$ was set, as the purity, SNR, and BER are affected by the intensity distribution of the beam. When a non-uniformly correlated high-order Bessel–Gaussian beam carrying the OAM state propagates in a turbulent atmosphere, the cumulative effect induced by the turbulence is assumed to be a pure phase perturbation effect on this beam [6]. Then, the CSD function of the non-uniformly correlated high-order Bessel–Gaussian beams propagating under conditions of atmospheric turbulence can be obtained as follows [26]:

$$\begin{aligned} W_T(\rho, \varphi_1, \varphi_2, z) &= W(\rho, \varphi_1, \varphi_2, z) \left\langle \exp\{i[\phi(\rho, \varphi_1) - \phi(\rho, \varphi_2)]\} \right\rangle \\ &= \left\langle E_T^*(\rho, \varphi_1, z) E_T(\rho, \varphi_2, z) \right\rangle \left\langle \exp\{i[\phi(\rho, \varphi_1) - \phi(\rho, \varphi_2)]\} \right\rangle \end{aligned} \quad (7)$$

Here, $E_T(\rho, \varphi, z)$ is the electric field of the beam in the receiver plane. With the help of the quadratic approximation of the wave structure function, the atmospheric turbulence disturbance term in the above formula can be obtained as follows:

$$\left\langle \exp\{i[\phi(\rho, \varphi_1) - \phi(\rho, \varphi_2)]\} \right\rangle = \exp\left\{-\frac{2\rho^2}{\rho_0^2} [1 - \cos(\varphi_1 - \varphi_2)]\right\} \quad (8)$$

Here, ρ_0 is the spatial coherence length of the atmospheric turbulence, as follows [43]:

$$\rho_0 = (0.545 C_n^2 k^2 z)^{-3/5}. \tag{9}$$

Here, the parameter C_n^2 is the turbulence structure constant, the value characterizing the strength of the atmospheric turbulence.

The OAM mode carried by the vortex beam inevitably encounters atmospheric turbulence after propagating over a long distance; the phase and complex amplitude of non-uniformly correlated Bessel–Gaussian beams are disturbed by the refractive index fluctuations of the turbulent atmosphere; the phase becomes extremely complicated; and the OAM states cannot maintain their original status. In order to facilitate the analysis of the signal and crosstalk, Fourier transform theory was applied. The electric field in the receiver plane $E_T(\rho, \varphi, z)$ can be written as a superposition of the plane waves with different OAM states; then, the complex-amplitude plane wave can be written as a coefficient and the term $\exp(il\varphi)$, and the CSD function $W_T(\rho, \varphi_1, \varphi_2, z)$ in the receiver plane can be rewritten as follows [13]:

$$W_T(\rho, \varphi_1, \varphi_2, z) = \sum_l \langle |a_l(\rho, z)|^2 \rangle \exp[-il(\varphi_1 - \varphi_2)] \tag{10}$$

Here, a_l is the expansion coefficient with the new OAM quantum number l . Then, the spatial distribution of intensity for a non-uniformly correlated high-order Bessel–Gaussian beam carrying the OAM modes can be determined as follows:

$$\langle |a_l(\rho, z)|^2 \rangle = \left(\frac{1}{2\pi}\right)^2 \int_0^{2\pi} \int_0^{2\pi} W_T(\rho, \varphi_1, \varphi_2, z) \exp[il(\varphi_1 - \varphi_2)] d\varphi_1 d\varphi_2 \tag{11}$$

Therefore, the received intensity of the non-uniformly correlated high-order Bessel–Gaussian beam carrying the OAM modes can be obtained as follows [13]:

$$I(z) = 2\pi \int_0^{D/2} \langle |a_l(\rho, z)|^2 \rangle \rho d\rho \tag{12}$$

Here, D is the diameter of the receiving aperture.

Substituting Equations (2), (6), (7), and (11) into Equation (12), we determined the received intensity of the OAM modes of non-uniformly correlated Bessel–Gaussian beams:

$$I(z) = \int p(v) I_l(\rho, z) dv \tag{13}$$

where

$$\begin{aligned} I_l(\rho, z) = & \frac{\pi k^2}{2z^2 [\beta_1^2 - (\beta_2 - \beta_3)^2]} \exp \left\{ -\frac{\alpha^2}{2w_0^2 [\beta_1^2 - (\beta_2 - \beta_3)^2]} \right\} \\ & \times \int_0^{D/2} I_{l_0} \left[\frac{\alpha k \rho}{2z(\beta_1 + \beta_2 - \beta_3)} \right] I_{l_0} \left[\frac{\alpha k \rho}{2z(\beta_1 - \beta_2 + \beta_3)} \right] I_{\Delta l} \left(\frac{2\rho^2}{\rho_0^2} \right) \\ & \times \exp \left\{ -\left[\frac{k^2}{2z^2 w_0^2 [\beta_1^2 - (\beta_2 - \beta_3)^2]} + \frac{2}{\rho_0^2} \right] \rho^2 \right\} \rho d\rho \end{aligned} \tag{14}$$

and $\Delta l = l_0 - l$, $\beta_1 = 1/w_0^2$, $\beta_2 = ik/2z$, $\beta_3 = ikv$.

The detection probability of the OAM mode for a non-uniformly correlated high-order Bessel–Gaussian beam propagating under conditions of atmospheric turbulence is defined as follows [13]:

$$P = \frac{I(z)}{\sum_{\Delta l=-\infty}^{\infty} I(z)} \quad (15)$$

where $I(z)$ describes the intensity of the signal OAM beam, and the term $\sum_{\Delta l=-\infty}^{\infty} I(z)$ denotes the intensity of both the signal OAM beam and the crosstalk OAM beams. To describe the channel loss and crosstalk of the OAM communication system, a signal-to-noise ratio (SNR) per bit of the OAM mode for a non-uniformly correlated high-order Bessel–Gaussian beam was introduced; it is shown below [18]:

$$\text{SNR} = \frac{I(z)}{\sum_{\Delta l=-\infty}^{\infty} I(z), (\Delta l \neq 0)} \quad (16)$$

here, the term $\sum_{\Delta l=-\infty}^{\infty} I(z), (\Delta l \neq 0)$ denotes the intensity of the crosstalk OAM beams. The average bit error rate (BER) is an important parameter used to measure signal quality for FSO communication systems. The average BER of non-uniformly correlated high-order Bessel–Gaussian beams under conditions of atmospheric turbulence can be expressed as follows:

$$\text{BER} = \frac{1}{2} \text{erfc} \left(\sqrt{\text{SNR} / 2} \right) \quad (17)$$

Equations (15)–(17) are the main analytical expressions used in this study. From Equation (14), it can be gleaned that the detection probability, SNR, and BER are affected by the difference of the signal OAM state and the crosstalk OAM states, beam width wavelength, receiver aperture diameter, and the strength of the turbulent atmosphere. The numerical results provide a convenient way of analyzing the performance of orbital angular momentum communication for a non-uniformly correlated high-order Bessel–Gaussian beam in a turbulent atmosphere.

3. Results and Discussion

In this section, we analyze the performance of an FSO communication system utilizing non-uniformly correlated high-order Bessel–Gaussian beams carrying the OAM state under conditions of atmospheric turbulence. The parameters were set as follows, unless otherwise indicated: $w_0 = 1$ cm, $r_c = 1$ cm, $l_0 = 1$, $\alpha = 10^3$ m⁻¹, $\lambda = 1550$ nm, $C_n^2 = 5 \times 10^{-15}$ m^{-2/3}, $D = 10$ mm, and $z = 500$ m.

Figure 1 shows the detection probability of the OAM mode for non-uniformly correlated high-order Bessel–Gaussian beam propagation in a turbulent atmosphere. As shown in Figure 1a, the detection probabilities of the topological charge difference $|\Delta l| = 1, 2,$ and 3 increase when propagation increases, and the detection probability for a large topological charge difference is smaller than that for a small topological charge difference. The detection probability of the signal OAM state for the topological charge difference $|\Delta l| = 0$ reduces slightly when the propagation distance increases. These results show that the power of the signal OAM states spreading to the neighbor OAM states is very small when the OAM state carried by non-uniformly correlated high-order Bessel–Gaussian beams is disturbed by a turbulent atmosphere; that is, high-order Bessel–Gaussian beams with a non-uniform correlation can be used to mitigate the perturbations caused by a turbulent atmosphere. Figure 1b shows that the signal OAM state at $|\Delta l| = 0$ has the most

power at the different propagation distances, the crosstalk of the OAM states appears in the neighboring modes for the topological charge difference $|\Delta l| = 1$, and the power of the other OAM states' crosstalk for the large topological charge difference is very low.

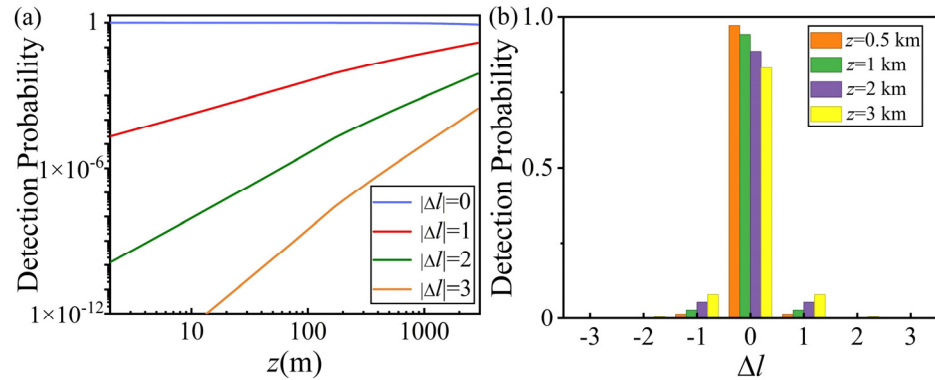


Figure 1. Detection probability of the OAM mode for non-uniformly correlated high-order Bessel–Gaussian beams in a turbulent atmosphere with different (a) topological charge differences $|\Delta l|$ and (b) propagation distances z .

Figure 2 shows the detection probability of the signal OAM state for non-uniformly correlated high-order Bessel–Gaussian beams affected by different receiving aperture diameters. As shown in Figure 2, the detection probability of the signal OAM state decreases at the different receiving aperture diameters ($D = 10$ mm, 20 mm, 30 mm, and 40 mm) when the propagation distance increases. At the same propagation distance, the detection probability of the signal OAM state limited by a small aperture is greater than it is when the receiver aperture is large. This result shows that the receiver aperture can be used to filter crosstalk from neighboring OAM states generated by a turbulent atmosphere. Therefore, choosing a suitably sized receiver aperture can effectively enhance the transmission quality of the signal OAM mode in the turbulent atmosphere channels.

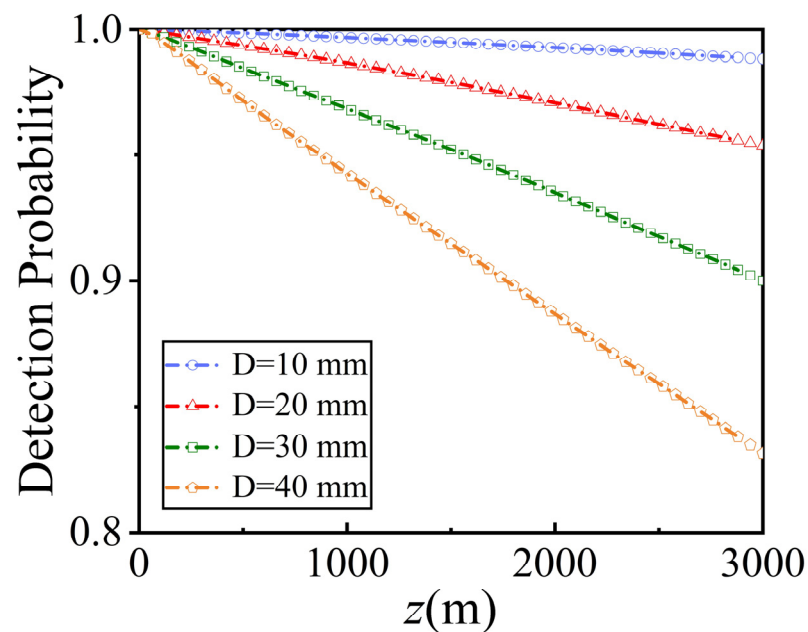


Figure 2. Detection probability of the signal OAM state for the non-uniformly correlated high-order Bessel–Gaussian beams at the different receiving aperture diameters (D).

Figure 3 shows the detection probability of the different signal OAM states carried by the non-uniformly correlated high-order Bessel–Gaussian beams propagating in a turbulent atmosphere; the topological charges l_0 of the signal OAM states are 1, 3, 5, and 7, respectively. As shown in Figure 3, the detection probabilities decrease when the propagation distance increases. The detection probabilities of the signal OAM state are the same at the near field; as the propagation distance further increases, the detection probabilities of the signal beam carrying the large OAM state are lower than those for the beam with the small OAM state. These results show that the non-uniformly correlated high-order Bessel–Gaussian beams carrying the large OAM states are affected easily by the turbulent atmosphere.

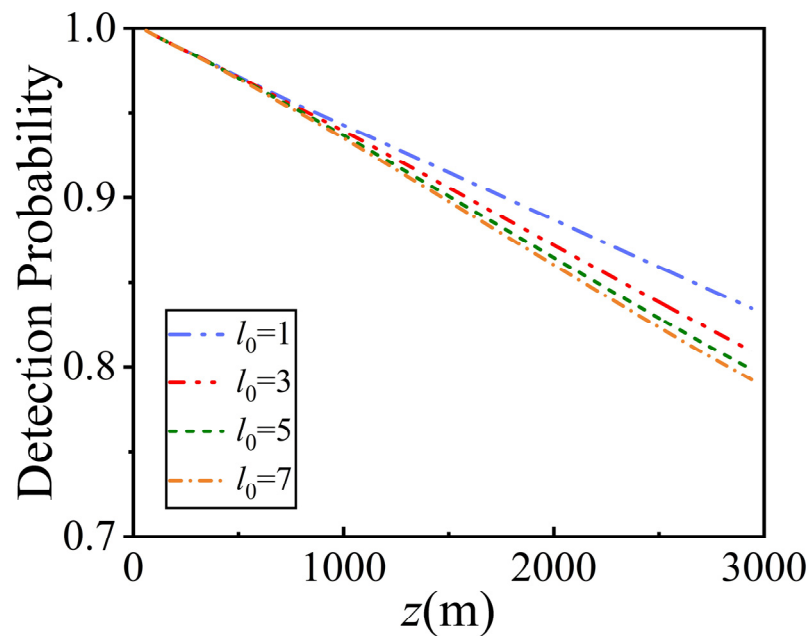


Figure 3. Detection probability of the different signal OAM states carried by the non-uniformly correlated high-order Bessel–Gaussian beams in a turbulent atmosphere.

Figure 4 shows the detection probability of the signal OAM state carried by the non-uniformly correlated high-order Bessel–Gaussian beams in a turbulent atmosphere for the different wavelengths (λ) studied. From Figure 4, it can be gleaned that, at the same propagation distance, the signal OAM state of the beam with a long wavelength has a high detection probability in the receiver plane. The results indicate that the long wavelengths have slower phase accumulation; thus, the disturbance of the signal OAM state by the turbulent atmosphere is slight, and the purity of the signal OAM state is higher. One can see that the OAM state carried by the non-uniformly correlated high-order Bessel–Gaussian beams at the wavelength of $\lambda = 1550$ nm propagating in a turbulent atmosphere is superior to that of the beams at the shorter wavelengths, and the wavelength $\lambda = 1550$ nm is also the atmospheric window in FSO communications.

Figure 5 shows the detection probability of the signal OAM state carried by the non-uniformly correlated high-order Bessel–Gaussian beams influenced by the beam width at the different propagation distances. As shown in Figure 5, the detection probability decreases when the propagation distance and beam width increase; this phenomenon can be attributed to the turbulent atmosphere having an accumulative effect as the propagation distance increases.

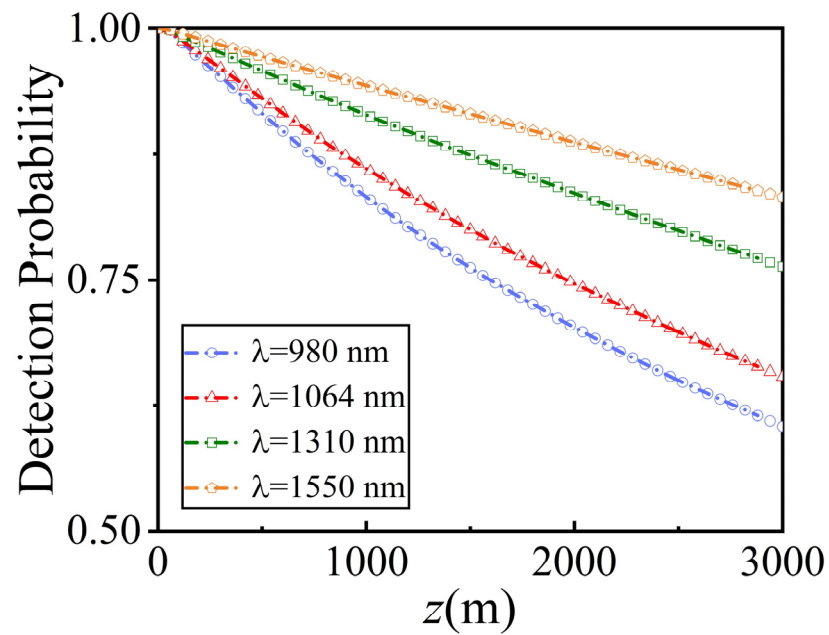


Figure 4. Detection probability of the signal OAM state carried by the non-uniformly correlated high-order Bessel–Gaussian beams in a turbulent atmosphere for the different wavelengths studied.

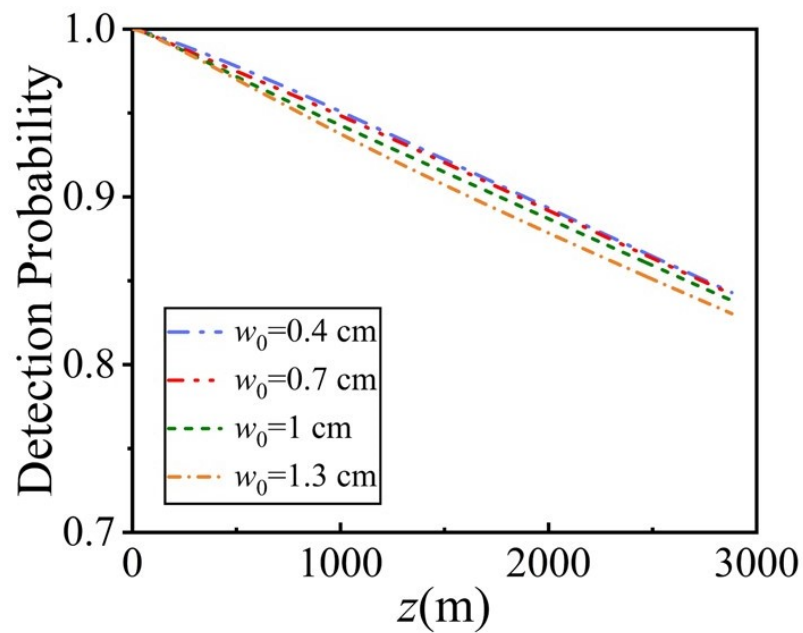


Figure 5. Detection probability of the signal OAM state carried by the non-uniformly correlated high-order Bessel–Gaussian beams in the turbulent atmosphere for the different beam widths analyzed.

Figure 6 illustrates the relationship between the SNR of the signal OAM state and the beam width of the non-uniformly correlated high-order Bessel–Gaussian beams propagating in an atmospheric turbulence channel at the propagation distance of $z = 0.5$ km, for which the topological charges l_0 of the signal OAM states are 1, 3, 5, and 7, respectively. As shown in Figure 6, the small-signal OAM state carried by the non-uniformly correlated high-order Bessel–Gaussian beam has a high SNR, and the non-uniformly correlated high-order Bessel–Gaussian beam carries a large topological charge l_0 ; as a result, the spots of the beams become large, and the signal OAM state induced by the turbulent atmosphere becomes serious. Therefore, the purity of the signal OAM state decreases, and the SNR is

large for the small topological charge under the same conditions; this result agrees well with Figure 3. The SNR of the signal OAM state is almost unchanged at a small beam width. As the beam width increases, the SNR of the signal OAM state decreases. These results agree well with the large spots of the beams influenced seriously by the turbulent atmosphere. The different signal OAM states have the same SNR when the non-uniformly correlated high-order Bessel–Gaussian beams have a very large beam width.

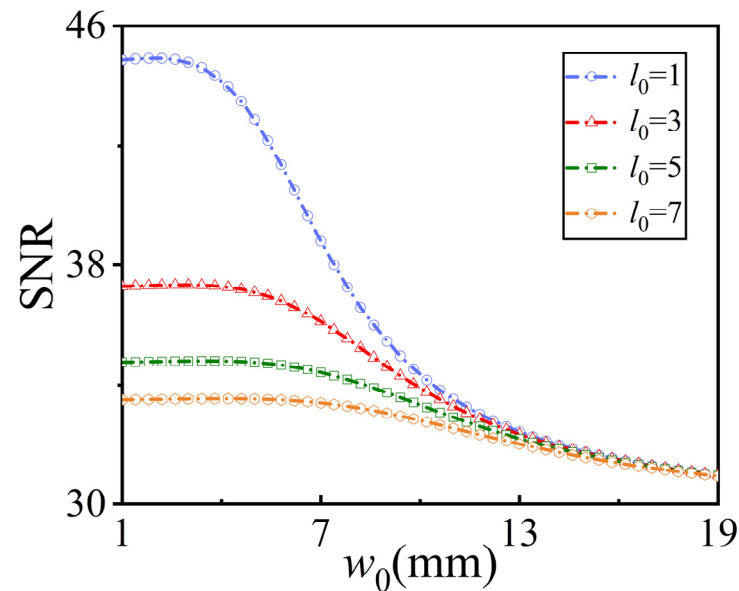


Figure 6. SNR of the different signal OAM states carried by the non-uniformly correlated high-order Bessel–Gaussian beams in a turbulent atmosphere against the beam width.

Figure 7 plots the average BER of the different signal OAM states carried by the non-uniformly correlated high-order Bessel–Gaussian beams in a turbulent atmosphere at a propagation distance of $z = 0.5$ km. As shown in Figure 6, the variation trend of the average BER of the signal OAM state is opposite to that of the SNR of the signal OAM state shown in Figure 6. This result agrees well with the low BER of the signal OAM state at a high SNR.

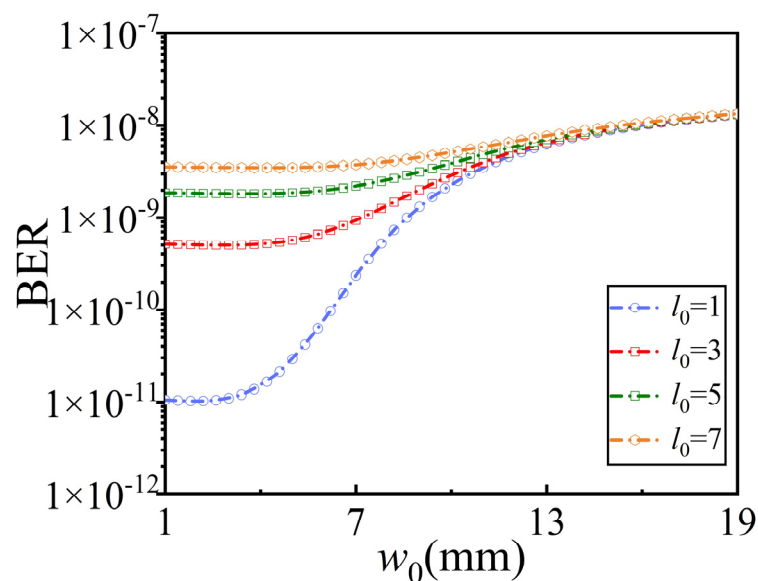


Figure 7. Average BER of the different signal OAM states carried by the non-uniformly correlated high-order Bessel–Gaussian beams in the turbulent atmosphere against the beam width.

Figure 8 shows the SNR and average BER of the signal OAM state carried by the non-uniformly correlated high-order Bessel–Gaussian beams affected by the strength of a turbulent atmosphere. As shown in Figure 8, the SNR of the signal OAM state decreases when the strength of the turbulent atmosphere and the beam width increase (see Figure 8a); this phenomenon can be interpreted as the purity of the signal OAM state decreasing due to the strong effect of the turbulent atmosphere. The variation trend of the average BER of the signal OAM state induced by the turbulent atmosphere is opposite to the SNR of the signal OAM state (see Figure 8b).

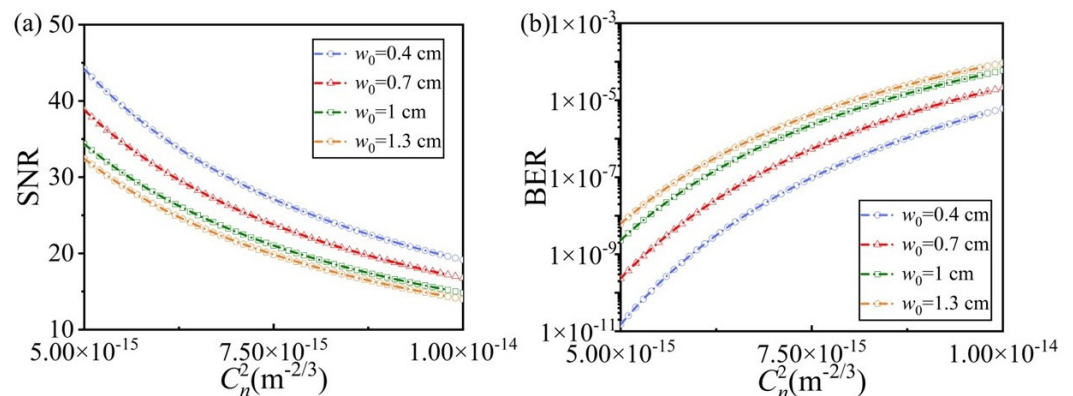


Figure 8. (a) SNR and (b) average BER of the signal OAM state carried by the non-uniformly correlated high-order Bessel–Gaussian beams with different beam widths against the strength of the turbulent atmosphere.

4. Conclusions

In summary, the detection probability, SNR, and average BER of the signal OAM state carried by non-uniformly correlated high-order Bessel–Gaussian beams in a turbulent atmosphere were derived. The theoretical calculations show that the detection probability of the signal OAM state decreases when the propagation distance, receiver aperture diameter, strength of the turbulent atmosphere, and topological charge increase and the wavelength decreases. The SNR and average BER of the signal OAM state are affected by the beam width. The BER of the signal OAM state decreases with an increase in the SNR when a non-uniformly correlated high-order Bessel–Gaussian beam propagating in a weak turbulent atmosphere has a small beam width. Non-uniformly correlated high-order Bessel–Gaussian beams carrying the OAM state might be very useful for FSO communications.

Author Contributions: Conceptualization, H.Z. and Y.Y.; writing—original draft preparation, Z.C. and Y.G.; writing—review and editing, Z.C. and H.Z.; supervision, Y.C. and Y.Y.; funding acquisition, Y.G., Y.C. and Y.Y. All authors have read and agreed to the published version of the manuscript.

Funding: This research was funded by the National Key Research and Development Program of China (Nos. 2022YFA1404800 and 2019YFA0705000) and the National Natural Science Foundation of China (NSFC) (Nos. 12192254, 11974219, 11974218, 12174227, 11904211, and 92250304).

Institutional Review Board Statement: Not applicable.

Informed Consent Statement: Not applicable.

Data Availability Statement: Data are contained within the article.

Conflicts of Interest: The authors declare no conflicts of interest.

References

1. Wang, J.; Yang, J.; Fazal, I.; Ahmed, N.; Yan, Y.; Huang, H.; Ren, Y.; Yue, Y.; Dolinar, S.; Tur, M.; et al. Terabit free-space data transmission employing orbital angular momentum multiplexing. *Nat. Photonics* **2012**, *6*, 488–496.

2. Bozinovic, N.; Yue, Y.; Ren, Y.; Tur, M.; Kristensen, P.; Huang, H.; Willner, A.E.; Ramachandran, S. Terabit-Scale Orbital Angular Momentum Mode Division Multiplexing in Fibers. *Science* **2013**, *340*, 1545–1548.
3. Lei, T.; Zhang, M.; Li, Y.; Jia, P.G.; Liu, N.; Xu, X.; Li, Z.; Min, C.; Lin, J.; Yu, C.; et al. Massive individual orbital angular momentum channels for multiplexing enabled by Dammann gratings. *Light Sci. Appl.* **2015**, *4*, e257.
4. Shen, Y.; Wang, X.; Xie, Z.; Min, C.; Fu, X.; Liu, Q.; Gong, M.; Yuan, X. Optical vortices 30 years on: OAM manipulation from topological charge to multiple singularities. *Light Sci. Appl.* **2019**, *8*, 90.
5. Wang, H.; Zhan, Z.; Hu, F.; Meng, Y.; Liu, Z.; Fu, X.; Liu, Q. Intelligent optoelectronic processor for orbital angular momentum spectrum measurement. *PhotonIX* **2023**, *4*, 9.
6. Paterson, C. Atmospheric turbulence and orbital angular momentum of single photons for optical communication. *Phys. Rev. Lett.* **2005**, *94*, 153901.
7. Anguita, J.A.; Neifeld, M.A.; Vasic, B.V. Turbulence-induced channel crosstalk in an orbital angular momentum-multiplexed free-space optical link. *Appl. Opt.* **2008**, *47*, 2414–2429.
8. Tyler, G.A.; Boyd, R.W. Influence of atmospheric turbulence on the propagation of quantum states of light carrying orbital angular momentum. *Opt. Lett.* **2009**, *34*, 142–144.
9. Rodenburg, B.; Lavery, M.P.J.; Malik, M.; O’Sullivan, M.N.; Mirhosseini, M.; Robertson, D.J.; Padgett, M.; Boyd, R.W. Influence of atmospheric turbulence on states of light carrying orbital angular momentum. *Opt. Lett.* **2012**, *37*, 3735–3737.
10. Acevedo, C.; Eshaghi, M.; Dogariu, A. Propagation of asymmetric optical vortex beams through turbulence and evolution of their OAM spectra. *J. Opt. Soc. Am. A* **2023**, *40*, 2135.
11. Wang, X.; Wang, Y.; Mao, S.; Yu, Y.; Gu, H.; Deng, D.; Song, Y.; Pang, F.; Zhuang, L.; Yang, S.; et al. Synthesizing the crosstalk between OAM modes of vortex beam by simultaneously propagation a probe vortex beam in free space. *Opt. Laser Technol.* **2023**, *165*, 109622.
12. Ju, P.; Fan, W.; Gao, W.; Li, Z.; Gao, Q.; Jiang, X.; Zhang, T. Atmospheric turbulence effects on the performance of orbital angular momentum multiplexed free-space optical links using coherent beam combining. *Photonics* **2023**, *10*, 634.
13. Chen, M.; Yu, L.; Zhang, Y. Signal/noise ratio of orbital angular momentum modes for a partially coherent modified Bessel-correlated beam in a biological tissue. *J. Opt. Soc. Am. A* **2017**, *34*, 2046–2051.
14. Ma, J.; Jiang, Y.; Tan, L.; Yu, S.; Du, W. Influence of beam wander on bit-error rate in a ground-to-satellite laser uplink communication system. *Opt. Lett.* **2008**, *33*, 2611–2613.
15. Mahdiah, M.H.; Pournoury, M. Atmospheric turbulence and numerical evaluation of bit error rate (BER) in free-space communication. *Opt. Laser Technol.* **2010**, *42*, 55–60.
16. Qiao, N.; Zhang, B.; Pan, P.; Dan, Y. Scintillation index and bit error rate of hollow Gaussian beams in atmospheric turbulence. *J. Mod. Opt.* **2011**, *58*, 939–944.
17. Liu, J.; Wang, P.; Zhang, X.; He, Y.; Zhou, X.; Ye, H.; Li, Y.; Xu, S.; Chen, S.; Fan, D. Deep learning based atmospheric turbulence compensation for orbital angular momentum beam distortion and communication. *Opt. Express* **2019**, *27*, 16671–16688.
18. Cheng, M.; Dong, K.; Shi, C.; Mohammed, A.H.T.; Guo, L.; Yi, X.; Wang, P.; Li, J. Enhancing Performance of Air–Ground OAM Communication System Utilizing Vector Vortex Beams in the Atmosphere. *Photonics* **2023**, *10*, 41.
19. Yu, J.; Zhu, X.; Wang, F.; Chen, Y.; Cai, Y. Research progress on manipulating spatial coherence structure of light beam and its applications. *Prog. Quant. Electron.* **2023**, *91–92*, 100486.
20. Li, J.; Chen, X.; McDuffie, S.; Najjar, S.M.A.M.; Rafsanjani, S.M.H.; Korotkova, O. Mitigation of atmospheric turbulence with random light carrying OAM. *Opt. Commun.* **2019**, *446*, 178–185.
21. Akbucak, V.; Aymelek, G.; Yolcu, B.; Kayam, O.; Ünal, O.; Gökçe, M.C.; Baykal, Y. Effect of partial coherence on signal-to-noise ratio performance of free space optical communication system in weak turbulence. *Opt. Commun.* **2022**, *518*, 128395.
22. Ricklin, J.C.; Davidson, F.M. Atmospheric optical communication with a Gaussian Schell beam. *J. Opt. Soc. Am. A* **2003**, *20*, 856–866.
23. Pan, P.; Zhang, B.; Qiao, N.; Dan, Y. Characteristics of scintillations and bit error rate of partially coherent rectangular array beams in turbulence. *Opt. Commun.* **2011**, *284*, 1019–1025.
24. Mays, J.; Gbur, G. Angular momentum of vector-twisted-vortex Gaussian Schell-model beams. *J. Opt. Soc. Am. A* **2023**, *40*, 1417.
25. Wang, H.; Liu, D.; Zhou, Z. The propagation of radially polarized partially coherent beam through an optical system in turbulent atmosphere. *Appl. Phys. B* **2010**, *101*, 361.
26. Zhu, Y.; Zhang, L.; Zhang, Y. Spiral spectrum of Airy–Schell beams through non-Kolmogorov turbulence. *Chin. Opt. Lett.* **2016**, *14*, 042101.
27. Wu, K.; Huai, Y.; Zhao, T.; Jin, Y. Propagation of partially coherent four-petal elliptic Gaussian vortex beams in atmospheric turbulence. *Opt. Express* **2018**, *26*, 30061–30075.
28. Liu, Y.; Chen, Y.; Wang, F.; Cai, Y.; Liang, C.; Korotkova, O. Robust far-field imaging by spatial coherence engineering. *Opto-Electron. Adv.* **2021**, *4*, 210027.
29. Xu, Y.; Xu, Y. Scintillation index and bit error rate of partially coherent twisted Gaussian beams in turbulent atmosphere. *Opt. Quantum Electron.* **2023**, *55*, 519.
30. Lajunen, H.; Saastamoinen, T. Propagation characteristics of partially coherent beams with spatially varying correlations. *Opt. Lett.* **2011**, *36*, 4104–4106.
31. Tong, Z.; Korotkova, O. Nonuniformly correlated light beams in uniformly correlated media. *Opt. Lett.* **2012**, *37*, 3240–3242.

32. Mei, Z.; Tong, Z.; Korotkova, O. Electromagnetic non-uniformly correlated beams in turbulent atmosphere. *Opt. Express* **2012**, *20*, 26458–26463.
33. Tong, Z.; Korotkova, O. Electromagnetic nonuniformly correlated beams. *J. Opt. Soc. Am. A* **2012**, *29*, 2154–2158.
34. Hyde M.; Bose-Pillai S.; Wood R. Synthesis of non-uniformly correlated partially coherent sources using a deformable mirror. *Appl. Phys. Lett.* **2017**, *111*, 101106. Zhou, X.; Zhou, Z.; Yuan, X. Research on performance of convex partially coherent flat-topped beams in vertical atmospheric turbulent paths. *Opt. Commun.* **2021**, *482*, 126577.
35. Lin, R.; Chen, M.; Liu, Y.; Zhang, H.; Gbur, G.; Cai, Y.; Yu, J. Measuring refractive indices of a uniaxial crystal by structured light with non-uniform correlation. *Opt. Lett.* **2021**, *46*, 2268–2271.
36. Yu, J.; Xu, Y.; Lin, S.; Zhu, X.; Gbur, G.; Cai, Y. Longitudinal optical trapping and manipulating rayleigh particles by spatial nonuniform coherence engineering. *Phys. Rev. A* **2022**, *106*, 033511.
37. Gu, Y.; Gbur, G. Scintillation of nonuniformly correlated beams in atmospheric turbulence. *Opt. Lett.* **2013**, *38*, 1395–1397.
38. Yang, X.; Fu, W. Propagation of radially polarized beams with a Hermite non-uniformly correlated array in free space and turbulent atmosphere. *Opt. Express* **2023**, *31*, 14403.
39. Dao, W.; Liang, C.; Wang, F.; Cai, Y.; Hoenders, B.J. Effects of Anisotropic Turbulence on Propagation Characteristics of Partially Coherent Beams with Spatially Varying Coherence. *Appl. Sci.* **2018**, *8*, 2025.
40. Zhou, X.; Zhou, Z.; Yuan, X. Research on performance of convex partially coherent flat-topped beams in vertical atmospheric turbulent paths. *Opt. Commun.* **2021**, *482*, 126577.
41. Zhao, Y.; Yan, Z.; Wang, Y.; Liu, L.; Zhu, X.; Guo, B.; Yu, J. Second-Order Statistics of Partially Coherent Beams with Laguerre Non-Uniform Coherence Properties under Turbulence. *Photonics* **2023**, *10*, 837.
42. Yan, Z.; Xu, Y.; Lin, S.; Chang, H.; Zhu, X.; Cai, Y.; Yu, J. Enhancing fiber-coupling efficiency of beam-to-fiber links in turbulence by spatial non-uniform coherence engineering. *Opt. Express* **2023**, *31*, 25680–25690.
43. Andrews, L.C.; Phillips, R.L. *Laser Beam Propagation through Random Media*, 2nd ed.; SPIE Press: Bellingham, Washington USA, 2005.

Disclaimer/Publisher’s Note: The statements, opinions and data contained in all publications are solely those of the individual author(s) and contributor(s) and not of MDPI and/or the editor(s). MDPI and/or the editor(s) disclaim responsibility for any injury to people or property resulting from any ideas, methods, instructions or products referred to in the content.